

Factors favorable to frequent extreme precipitation in the upper Yangtze River Valley

Baoqiang Tian · Ke Fan

Received: 4 October 2012 / Accepted: 6 May 2013
© Springer-Verlag Wien 2013

Abstract Extreme precipitation events in the upper Yangtze River Valley (YRV) have recently become an increasingly important focus in China because they often cause droughts and floods. Unfortunately, little is known about the climate processes responsible for these events. This paper investigates factors favorable to frequent extreme precipitation events in the upper YRV. Our results reveal that a weakened South China Sea summer monsoon trough, intensified Eurasian-Pacific blocking highs, an intensified South Asian High, a southward subtropical westerly jet and an intensified Western North Pacific Subtropical High (WNPSH) increase atmospheric instability and enhance the convergence of moisture over the upper YRV, which result in more extreme precipitation events. The snow depth over the eastern Tibetan Plateau (TP) in winter and sea surface temperature anomalies (SSTAs) over three key regions in summer are important external forcing factors in the atmospheric circulation anomalies. Deep snow on the Tibetan Plateau in winter can weaken the subsequent East Asian summer monsoon circulation above by increasing the soil moisture content in summer and weakening the land–sea thermal contrast over

East Asia. The positive SSTA in the western North Pacific may affect southwestward extension of the WNPSH and the blocking high over northeastern Asia by arousing the East Asian-Pacific pattern. The positive SSTA in the North Atlantic can affect extreme precipitation event frequency in the upper YRV via a wave train pattern along the westerly jet between the North Atlantic and East Asia. A tripolar pattern from west to east over the Indian Ocean can strengthen moisture transport by enhancing Somali cross-equatorial flow.

1 Introduction

The upper Yangtze River Valley (YRV) is prone to extreme climatic events, especially floods and droughts (Wang et al. 2012). These events can cause great damage to China's economy, water resources and ecosystem, as well as loss of human life and damage to property. For example, between autumn 2009 and winter 2010, a prolonged drought occurred in southwestern China, in the upper YRV. Subsequently, southwestern China experienced extreme summer rainstorms in 2010 and 2011, which caused huge economic losses. Unfortunately, little is known about the reasons for such extreme precipitation events. This paper seeks to fill this knowledge gap by identifying the characteristics of atmospheric circulation that are related to the frequency of extreme precipitation events in the upper YRV.

Previous research has focused on the variability of extreme precipitation in the middle and lower reaches of the YRV (Su et al. 2006a, b; Becker et al. 2008; Ren et al. 2010; You et al. 2011) rather than the upper YRV. Extreme precipitation in the YRV over the past 60 years has increased significantly, with the most significant increases occurring in the middle and lower reaches of the YRV.

Responsible editor: B. Ahrens.

B. Tian · K. Fan (✉)
Institute of Atmospheric Physics, Chinese Academy of Sciences,
Beijing 100029, China
e-mail: fanke@mail.iap.ac.cn

B. Tian
University of Chinese Academy of Sciences, Beijing 100049,
China

K. Fan
Key Laboratory of Regional Climate-Environment for East Asia,
Chinese Academy of Sciences, Beijing 100029, China

Since the mid-1980s, the extreme precipitation events in the upper YRV have occurred with greater frequency in June rather than in July (Su et al. 2006a). In most parts of China, no statistically significant change has been observed in heavy rain intensity, although a significant positive trend in total summer rainfall over the YRV has been detected (Zhai et al. 2005).

Atmospheric circulation anomalies can cause extreme rainfall events. Previous studies have shown that increasing anticyclonic circulation and geopotential height anomalies, along with rapid warming over the Eurasian continent, have contributed to changes in climate extremes in China (You et al. 2011). Certain weather systems and strengthened water vapor fluxes may facilitate the occurrence of rainstorms in the Sichuan–Chongqing region (Chen et al. 2010; Mao et al. 2010).

Because of the complicated topography of the YRV, its patterns of extreme precipitation show pronounced spatial heterogeneity. In contrast to the abundant research on extreme precipitation events in the middle and lower reaches of YRV, few studies have been conducted on extreme precipitation events in the upper YRV. This paper presents an examination of the interannual variation of extreme precipitation event frequency (EPF) in the upper YRV and a discussion of the types of atmospheric circulation that are favorable to EPF. The effects of the snow depth over the eastern Tibetan Plateau (TP) in winter and sea surface temperature anomalies (SSTAs) in summer on the EPF in the upper YRV are also examined in this paper.

2 Data and methodology

2.1 Data sources

The primary data sets used consist of daily observations of precipitation and snow depth from 756 weather stations monitored by the China Meteorological Administration (CMA). Monthly mean atmospheric data sets with $2.5^\circ \times 2.5^\circ$ horizontal resolution from the National Centers for Environmental Prediction and the National Center for Atmospheric Research (NCEP/NCAR) were also used. We selected 126 stations along the upper YRV with summer precipitation data, and 66 stations on the Tibetan Plateau with winter snow depth data, both spanning the 1961–2009 period. Stations with missing data were rejected. Figure 1a shows the spatial distribution of the stations in the upper YRV.

A heavy rain day at an observation station is defined as one with total precipitation >50 mm. An absolute threshold of precipitation is not suitable for every station. For this reason, the most commonly used international percentile method was chosen to define the extreme precipitation threshold (Plummer et al. 1999; Manton et al. 2001; Zhai

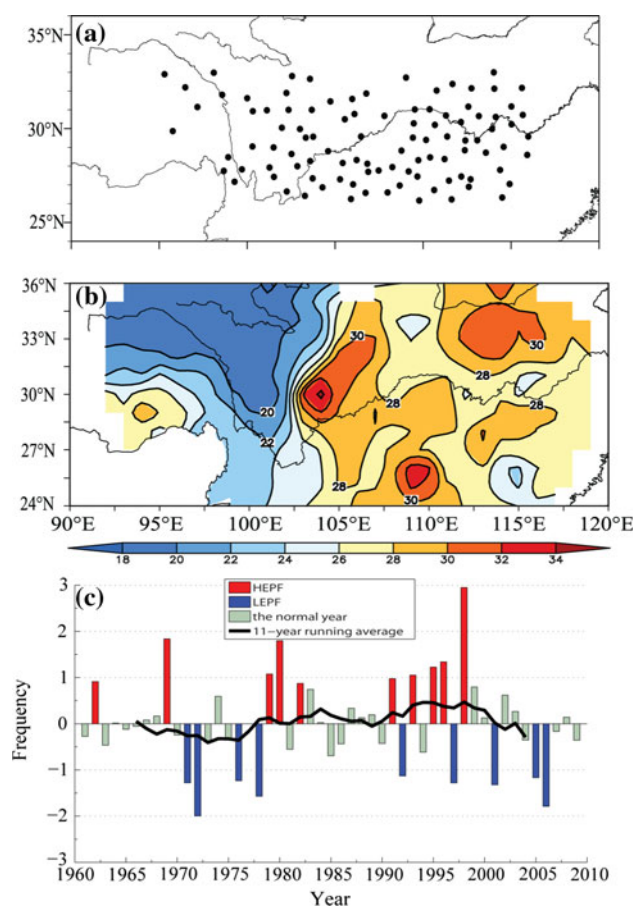


Fig. 1 Spatial and temporal distribution of EPF in the upper YRV. **a** Spatial distribution of meteorological stations in the upper YRV; **b** the proportion of 95th percentile precipitation contribution to the summer climatological precipitation during 1961–2009 in the upper YRV (unit: %); **c** variations of JJA EPF in the upper YRV from 1961 to 2009, normalized and detrended

et al. 2005). We defined this threshold for a station based on the daily precipitation in summer over the 1961–2009. First, daily precipitation amounts >0.1 mm were ranked in ascending order for each station. The precipitation amount at the 95th percentile was defined as the extreme precipitation event threshold for the station. If a day's rainfall at that station exceeded that threshold, that day was recorded as an extreme precipitation event. EPF indicates the number of days at the station characterized by extreme precipitation. As a result, the extreme precipitation threshold varies by station and is between 15.7 and 74.1 mm in the upper YRV. This threshold is close to the classification of heavy rain (50 mm/day) at some stations but is close to the classification of moderate rain (10–24.9 mm/day) at other stations. This demonstrates the advantage of using different thresholds that can accurately represent extreme precipitation at different stations.

The contribution of extreme precipitation to the summer climatological precipitation is shown in Fig. 1b. The

contribution of the 95th-percentile precipitation in the upper YRV to the summer climatological precipitation is 27 %. Figure 1b shows that the proportion of extreme precipitation exceeds 28 % in most of the middle reach of the YRV, while the contribution of extreme precipitation to summer climatological precipitation in the upper YRV is approximately 18–22 %. These proportions suggest that EPF in the upper YRV plays an important role in local floods and droughts and is correlated to the mean summer precipitation. The coefficient of correlation between the variation in EPF and total summer precipitation in the upper YRV is 0.76. Therefore, factors favorable to EPF in the upper YRV are stressed in this paper.

Atmospheric instability plays a key role in the occurrence of extreme precipitation events. The *K* index, a diagnostic factor for heavy rainfall, represents the stability of the atmosphere and is defined as follow:

$$K = (T_{850\text{hPa}} - T_{500\text{hPa}}) + (T_{d850\text{hPa}} - (T_{700\text{hPa}} - T_{d700\text{hPa}})),$$

where T_i is the air temperature at the i th level and $(T_d)_j$ is the dew point temperature at the j th level (Chen et al. 2012). A large value of the *K* index generally favors more frequent occurrences of heavy rainfall events.

3 Interdecadal and interannual variations in summer extreme precipitation event frequency

3.1 Interdecadal and interannual variation of summer EPF

The summer EPF in the upper YRV exhibits interdecadal and interannual variability (Fig. 1c). The 11-year running average of summer EPF during 1961–2009 shows that it decreased from the 1960s to the mid-1970s and then increased from the mid-1980s to the mid-1990s. The EPF has decreased since the late 1990s. The interannual variability of EPF in the upper YRV differs from that in the lower YRV, and the coefficient of correlation between the EPF in the upper YRV and the EPF in the lower YRV is 0.38. Actually, the characteristics of the anomalous atmospheric circulation associated with the EPF in the upper YRV bear some similarities to those associated with the EPF in the lower YRV, but they are also different in some respects. Therefore, it is imperative to understand the cause of summer EPF variation in the upper YRV.

3.2 Identifying years with high and low frequencies of extreme precipitation events

To explore the relationship between EPF interannual variation in the upper YRV and related atmospheric

circulations, we performed a composite analysis. In this analysis, the EPF in the upper YRV from 1961 to 2009 was normalized and detrended to capture its interannual time scale. The years in which the average EPF was 0.8 standard deviation above the mean for the period 1961–2009 were defined as high EPF (HEPF), and the years in which the average EPF was below -0.8 standard deviation were defined as low EPF (LEPF). Compared with 0.5 standard deviation of the average EPF, the overall EPF is very abnormal. Figure 1c shows that there were 10 HEPF years (1962, 1969, 1979, 1980, 1982, 1991, 1993, 1995, 1996, and 1998) and 9 LEPF years (1971, 1972, 1975, 1978, 1992, 1997, 2001, 2005, and 2006). We investigated the differences in the summer atmospheric circulations between the HEPF and LEPF years.

4 Factors favoring frequent extreme precipitation in the upper YRV

In this section, we focus on analyzing the processes and factors favorable to frequent extreme precipitation events in the upper YRV, especially the major atmospheric circulation processes and the influence of the snow depth in the eastern TP and summer SSTAs on these processes.

4.1 WNPSH and South Asian High

The WNPSH and South Asian High (SAH) have strong influences on the summer climate system in China (Tao and Zhu 1964; Jiang et al. 2011). When the WNPSH is abnormally south and west, strong southerly water vapor transport anomalies shift toward the YRV and its southern area (Liu and Ding, 2009). Previous research has shown that there is a significant positive correlation between SAH intensity and precipitation anomalies in the YRV (Zhang and Wu 2001). The variations in SAH and WPSH, as well as their interrelationship, can be well illustrated by the first SVD mode of 100- and 500-hPa geopotential heights, in which the SAH and the WPSH vary synchronously (Jiang et al. 2011). Figure 2a shows the characteristics of these two systems in the HEPF and LEPF years. In HEPF years, the WNPSH is shifted far southwestward, and the western end of the 5,860-geopotential-meter (gpm) contour line extends west of 109°E. Meanwhile, the SAH is enhanced that can intensify the upper-level divergence and low-level convective motion over the upper YRV. As a result, the southern part of China is under the control of the WNPSH, and more water vapor from the western North Pacific is transported westward to the upper YRV. In LEPF years, the WNPSH is shifted northeastward, and the SAH is simultaneously weakened. The western end of the 5,860-gpm contour line is located west of 119°E, as shown in Fig. 2a.

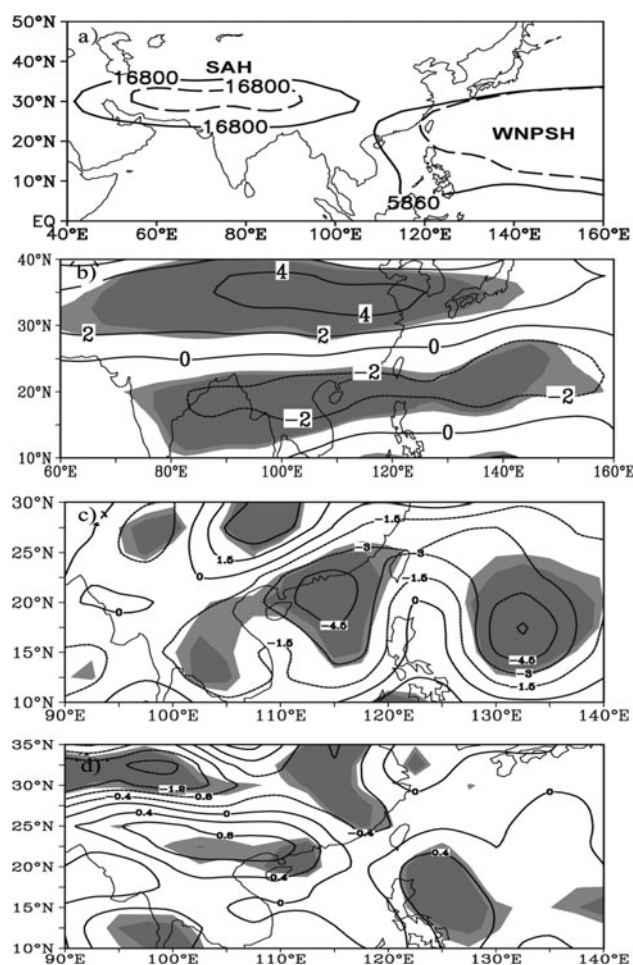


Fig. 2 Composite difference of the atmospheric circulation in JJA between HEPF and LEPF years. **a** Positions of WNPSH (5,860 gpm) and SAH (16,800 gpm) in JJA for HEPF years (solid line) and the LEPF years (dashed line); **b** zonal wind field at 200 hPa; **c** relative vorticity at 850 hPa; **d** horizontal divergence at 850 hPa (unit: 10^{-6} s^{-1}) Light and dark shaded areas are over 90 and 95 % confidence level by *t* test, respectively

Consequently, a large amount of water vapor from the western North Pacific is not transported to the upper YRV because of the weak ascending flow. Therefore, the westward extension of WNPSH and the eastward extension of SAH are important factors in the frequency of extreme precipitation events in the upper YRV.

4.2 East Asian subtropical westerly jet

As a summer monsoon component, the East Asian subtropical jet can affect summer precipitation over the YRV by modulating the location of the SAH and WNPSH. In general, a southward East Asian subtropical westerly jet can intensify the SAH, which produces ascending flow over the YRV, and a northward East Asian subtropical westerly jet can weaken the SAH, which produces descending flow over the YRV (Liao et al. 2004).

Figure 2b depicts features of the zonal wind at 200 hPa. In HEPF years, the center of the East Asian subtropical westerly jet shifts dramatically southward. This is characterized by a westerly wind anomaly dominating the YRV and an easterly wind anomaly in the region 10°N – 20°N . Such a wind field distribution can strengthen the anticyclonic circulation of the SAH, which intensifies upper-level divergence and low-level convective motion over the YRV. In LEPF years, the features of the wind fields are almost the opposite of those in HEPF years. The center of the westerly jet shifts northward, and an east wind anomaly prevails in the upper layers over the YRV.

4.3 Eurasian–Pacific blocking highs and Australian high

In HEPF years, two blocking high anomalies at high latitudes dominate Eurasia at 500 hPa (the figure is not shown). One is centered over the eastern Ural Mountains and the other is located over the western Sea of Okhotsk, together with a trough anomaly over Western Europe. This circulation pattern can facilitate cold air from high latitudes moving southward and westward to the upper YRV. Negative geopotential height anomalies across the YRV and its north side are concurrent with a positive anomaly of geopotential height in the tropical western Pacific during HEPF years. There is an alternating $+ - +$ wave train distribution of geopotential height anomalies at 500 hPa, from low to high latitudes over the East Asian coast. This distribution corresponds to a southward and enhanced WNPSH, a decrease in geopotential height from the YRV to parts of northern China, and an enhanced Okhotsk high, respectively. Such meridional atmospheric circulation anomalies over the East Asian coast are beneficial for abundant rainfall over the entire YRV (Liu et al. 2008). Furthermore, the Australian high is enhanced in HEPF years. As some research has indicated, this high can play a key role in summer rainfall over the YRV (Xue et al. 2003; Wang and Fan 2005; Fan 2006; Wang and Fan 2006; Liu et al. 2008; Sun et al. 2009; Zhou 2011). These results show that when the Australian high and the associated cross-equatorial flow strengthen and the trade winds over the tropical western and middle Pacific weaken, convective activity near the Philippine Sea is suppressed and a Rossby wave train is excited from East Asia to the North Pacific to the western North American coast. This results in southward displacement of the WNPSH. In addition, the intensified cross-equatorial flow over Australia can increase water vapor in the upper YRV.

4.4 The South China Sea summer monsoon trough

The South China Sea summer monsoon trough, which is an important monsoon system, is defined as the monsoon

convergence zone between the summer southwest monsoon and easterly wind to the southwest of the WNPSH. An anomalously strong or weak monsoon trough can affect the South China Sea summer monsoon anomaly, thus affecting precipitation anomalies in East Asia. Because the monsoon trough has strong convergence, its relative vorticity can be used as a measure of its intensity. Previous studies have shown that a continuously weak South China Sea summer monsoon trough not only causes more rainfall in the middle and lower YRV but also influences remote atmospheric circulation via atmospheric teleconnection (Li and Pan 2007). Variability of the tropical monsoon is associated with subtropical monsoon precipitation through the East Asian–Pacific meridional teleconnection or the Pacific–Japan wave train (Nitta 1987; Huang and Li 1988). Observational data analysis shows that on an interannual scale, the monsoons and rainfall over the middle and lower YRV have an out-of-phase relationship with those over the South China Sea during June and July (Jin and Zhao 2012). Here, we address the relationship between the South China Sea summer monsoon trough and EPF in the upper YRV. Figure 2c shows composite differences in the relative vorticity at 850 hPa in summer. A zone of negative relative vorticity is observed from the Arabian Sea, across the Indian subcontinent, across the Bay of Bengal and the Indochinese peninsula, to the South China Sea and the Philippine Sea. This indicates that the South China Sea summer monsoon trough becomes weaker than normal in HEPF years. Such an anomalous monsoon trough results in weak convergence in lower layers, hampering development of convection patterns. Horizontal divergence features at 850 hPa over the South China Sea (Fig. 2d) show weak convection in HEPF years. Under these conditions, anomalously strong convergence dominates the upper YRV, and to its south and north sides, abnormal divergence zones exist. Consequently, the weaker South China Sea summer monsoon trough often results in more frequent extreme precipitation in the upper YRV.

4.5 Characteristics of water vapor flux transport

Figure 3a shows composite differences in the vertically integrated summer water vapor flux transport between HEPF and LEPF years. In HEPF years, divergence of vertically integrated water vapor flux expands to northern Australia, the Bay of Bengal and the western North Pacific, while convergence of this flux extends from the North Indian Ocean to the Arabian Sea. This indicates that water vapor transported by the Somali cross-equatorial flow is hampered over the Arabian Sea and Indian Peninsula. The cross-equatorial flow over Australia is intensified along with the enhanced Australian high, which brings more water vapor into the Bay of Bengal and the western North

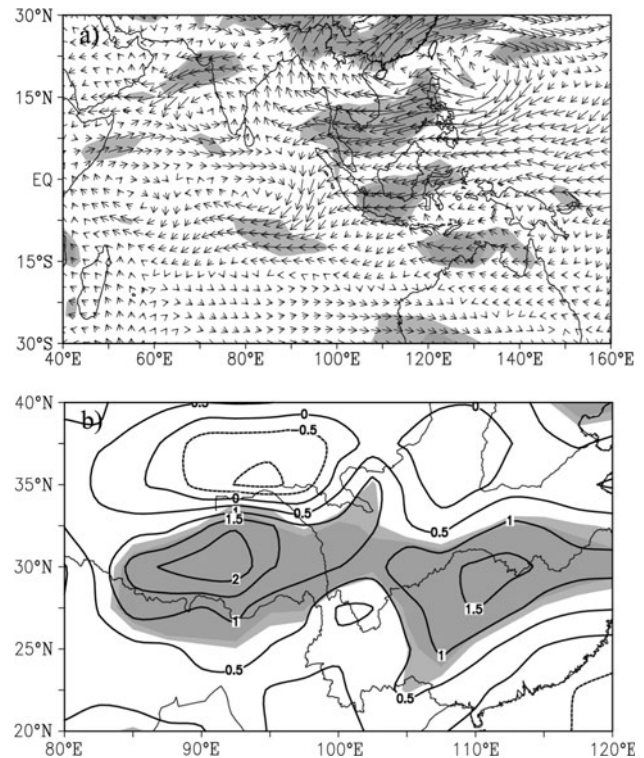


Fig. 3 Composite difference of **a** vertically integrated water vapor flux and **K** index in JJA between HEPF and LEPF years. *Light and dark shaded areas are over 90 and 95 % confidence level by t test, respectively*

Pacific (Fig. 3a). Subsequently, water vapor from the Bay of Bengal turns north toward the upper YRV, providing favorable conditions for extreme precipitation events. At the same time, enhanced easterly flow south of the WNPSH can transport moisture from the western North Pacific to the upper YRV. The composite difference **K** index in JJA between HEPF and LEPF years is shown in Fig. 3b. The **K** index significantly increases in the upper YRV, which indicates that the atmosphere stratification becomes very unstable. Under such circulation conditions, moisture ascends over the upper YRV, and more extreme precipitation events occur. Therefore, water vapor over northern Australia and divergence over the Bay of Bengal and western North Pacific contribute to more extreme precipitation events in the upper YRV.

4.6 Effect of the winter snow depth anomaly over the eastern TP on the EPF

It has been shown that snow anomalies over the Tibetan Plateau change soil moisture and surface temperature initially through melting of snow, which alters heat, moisture and radiation fluxes from the surface to the atmosphere. Abnormal circulation conditions induced by surface flux changes may in turn affect underlying surface properties.

This long-term interaction between wet surfaces and the atmosphere is important to subsequent climate change (Qian et al. 2003a, b). Studies have confirmed that a heavy snow over the Tibetan Plateau is positively correlated to heavy subsequent summer precipitation in the YRV (Qian et al. 2003a, b; Ding et al. 2009). Numerical and theoretical evidences indicate that anomalously low Tibetan Plateau snow cover can force positive geopotential height anomalies in the upper troposphere and weaken jet streams across eastern Asia and the northwestern Pacific (Wu et al. 2011). Moreover, anomalies in the Tibetan Plateau snow depth cause anomalies in air temperature and its contrast between the Indian Ocean and the continent, producing an SAH anomaly (Yu and Hu 2008). High snowmelt results in surface cooling over the Tibetan Plateau and neighboring regions and high-pressure anomalies that cause a southwestward extension of the western Pacific subtropical high during the subsequent summer. In addition, the increased surface moisture supply provides more energy for the development of the eastward-migrating low-level vortex over the eastern flank of the plateau. Both factors lead to a wetter summer in the vicinity of the YRV (Zhang et al. 2004).

There is a positive correlation between the EPF and winter snow depth on the eastern TP (the figure is not shown). Therefore, when the winter snow depth on the eastern TP is deeper than normal, extreme precipitation events in the upper YRV during the subsequent will be more frequent than normal. What is the mechanism behind this connection? To answer this question, a snow depth anomaly index (SDAI) is defined as the average snow depth anomaly of the significant region (30°N–33°N, 92°E–96°E) on the eastern TP. The relationship between the seasonal difference in soil moisture and the winter snow depth anomaly index (SDAI) is shown in Fig. 4a and b. Due to melting of the snow on the eastern TP, the soil moisture over the YRV increases significantly in spring and summer, which decreases the surface temperature and weakens the spring and summer land–sea thermal contrast over East Asia. A weak Asian summer monsoon appears in the subsequent summer, accompanied by the southwestward extension of WNPSH, strengthening of the SAH and the southward westerly jet, and strong atmospheric ascending motion over the upper YRV (see Fig. 4c). These atmospheric circulation anomalies increase atmospheric instability and enhance convergence of moisture over the upper YRV, thereby producing more frequent extreme precipitation events.

4.7 The effect of summer SSTA on the atmosphere circulation associated with extreme precipitation

Anomalies of atmospheric circulation can influence the SSTA. In turn, the SSTA in key areas can bring about

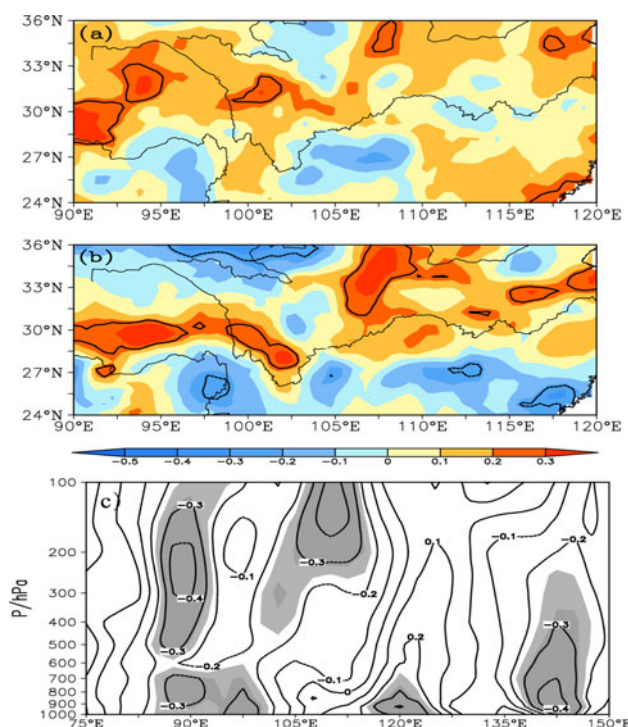


Fig. 4 Correlation coefficients between the winter SDAI and **a** the soil moisture seasonal difference between spring and winter; **b** the soil moisture seasonal difference between summer and spring; **c** the JJA vertical velocity averaged along 20°N–37°N. Light and dark shading indicates 90 and 95 % confidence level, respectively

anomalies of atmospheric circulation and thermal convection. Therefore, air–sea interactions play an important role in understanding short-term climate dynamics and climate prediction. In this section, we analyze the effect of summer SSTA on the atmospheric circulation associated with extreme precipitation. Figure 5a shows correlation coefficients between the summer EPF and the SSTA in summer. There are three key areas of SSTAs that are closely correlated with the summer EPF. Three SSTA indexes have been defined by the regional mean SSTA that lie in the western North Pacific (142°E–156°E, 22°N–28°N), the North Atlantic Ocean (10°W–24°W, 44°N–50°N; 2°W–12°W, 62°N–68°N; 6°W–12°W, 72°N–76°N) and the South Indian Ocean (106°E–114°E, 16°S–36°S; 46°E–52°E, 36°S–42°S; 64°E–84°E, 20°S–26°S) (see Fig. 5a). The influence of SSTAs over these key areas on the atmospheric circulations associated with extreme precipitation has been discussed in this section. To isolate the effect of other SSTAs over key areas, the partial correlation method was used in the analysis. Figure 5b shows the partial correlation coefficients between the geopotential height field at 500 hPa in JJA and the western North Pacific SSTA index. The positive SSTA in the western North Pacific may affect the blocking high over northeastern Asia and the southwestward WNPSH by arousing the East Asia–

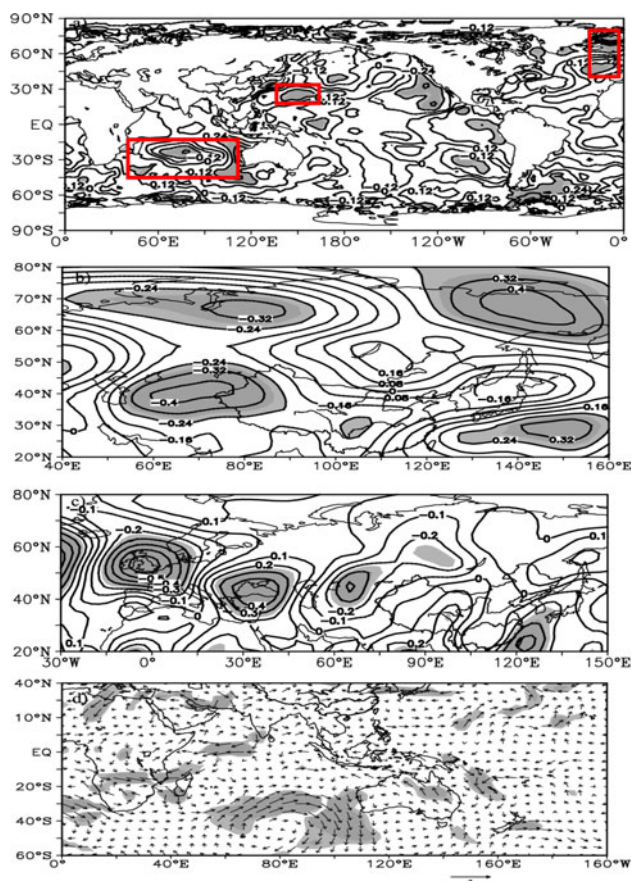


Fig. 5 The relationship between the summer SSTA and the atmospheric circulation. **a** Correlation coefficients between the summer EPF and the summer SSTA; partial correlation coefficients (**b**) between the geopotential height field at 500 hPa in JJA and the SSTA index over Western North Pacific Ocean; **c** coefficients between the meridional wind at 200 hPa in JJA and the SSTA index over North Atlantic Ocean; **d** between the horizontal wind at 850 hPa in JJA and the SSTA index over South India Ocean. The shading indicates 90 and 95 % confidence level

Pacific teleconnection pattern (EAP) (Lu and Huang 1998). In Fig. 5c, there is a wave train pattern along the westerly jet between the North Atlantic and East Asia, which may be aroused by the tripolar pattern of the SSTA in the North Atlantic. The wave train explains why the SSTA in the North Atlantic can affect the extreme precipitation in the upper YRV (Sung et al. 2006; Zhu et al. 2011; Tian and Fan 2012). In the Indian Ocean, the key area of the SSTA also has a tripolar pattern from west to east, which can strengthen moisture transport by enhancing Somali cross-equatorial flow (see Fig. 5d). Most of this branch moisture is converged in the Arabian Sea, and the rest of it enters into the Bay of Bengal and provides the water vapor for extreme precipitation events in the upper YRV (Xu and Fan 2012).

Insignificant correlations were detected between the winter SDAI and the three indexes of SSTA over the

regions: the correlation coefficients are 0.14, 0.08 and 0.03. That is, the Tibetan Plateau snow depth should be viewed as an independent external forcing factor that affects the summer rainfall in East Asia (Ding et al. 2009). Therefore, the winter snow depth over the TP and the summer SSTAs over key regions contribute to EPF in the upper YRV.

5 Conclusions and discussion

The analysis results presented in this paper indicate that extreme summer precipitation events in the upper YRV exhibit remarkable and distinct interdecadal and interannual variations. These changes are caused by anomalies of atmospheric circulation. The winter snow depth over the eastern TP and SSTAs are important external forcing factors for atmospheric circulation anomalies. Figure 6 shows schematic processes of probable influence, including the type of atmospheric circulation favorable for frequent extreme precipitation events in the upper YRV. Increased soil moisture due to melting snow decreases the surface temperature and weakens the spring and summer land–sea thermal contrast. A weak Asian summer monsoon trough occurs during the subsequent summer, accompanied by the southwestward extension of the WNPSH, strengthening of the SAH and the southward extension of the westerly jet, as well as strong atmospheric ascending motion over the upper YRV. These atmospheric circulation anomalies increase atmospheric instability and enhance the convergence of moisture over the upper YRV, resulting in more frequent extreme precipitation events in the upper YRV.

In summer, SSTAs over three key regions of the western North Pacific, the North Atlantic and the South Indian Ocean, can influence summer atmospheric circulation related to EPF in the upper YRV. The positive SSTA in the western North Pacific may affect the southwestward extension of the WNPSH and the blocking high over the northeastern Asia by arousing the EAP pattern (Lu and Huang 1998, see Fig. 5b). The SSTA in the North Atlantic can affect EPF in the upper YRV via a wave train pattern along the westerly jet between the North Atlantic and East Asia (see Fig. 5c, Sung et al. 2006; Zhu et al. 2011; Tian and Fan 2012). A tripolar pattern from west to east over the Indian Ocean can strengthen moisture transport by enhancing Somali cross-equatorial flow. Most of this branch moisture is converged in the Arabian Sea, and the rest of it enters into the Bay of Bengal and provides the water vapor for extreme precipitation events in the upper YRV (see Fig. 5d, Xu and Fan 2012).

The characteristics of the anomalous atmospheric circulation associated with the frequent EPF in the upper YRV bear some similarities to those in the lower YRV, but they are also different in some respects. According to our

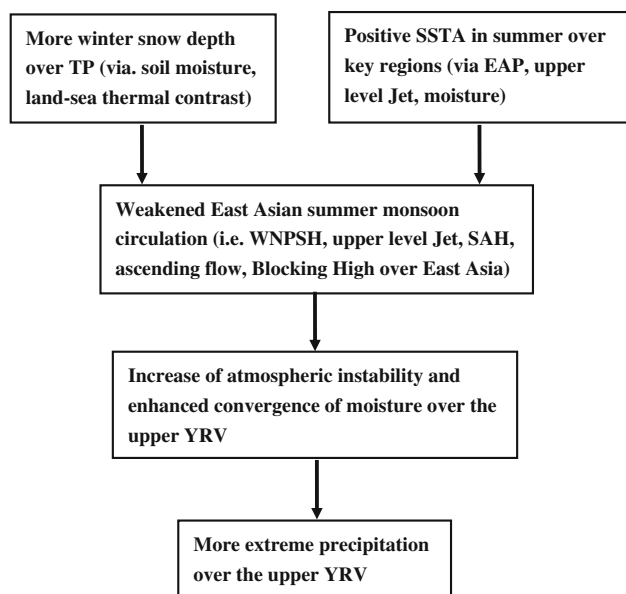


Fig. 6 Flowchart of probable mechanisms of summer EPF in the upper YRV

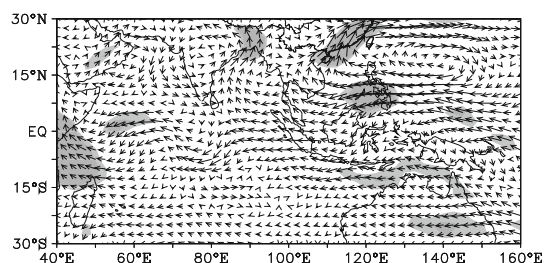


Fig. 7 Composite difference of water vapor flux in JJA between HEPF and LEPF years in the lower YRV (unit: $\text{kg m}^{-1} \text{s}^{-1}$). Light and dark shaded areas are over 90 and 95 % confidence level by *t* test, respectively

research, the moisture sources for extreme precipitation events in the lower reaches of the YRV differ considerably from those in the upper YRV. In HEPF years in the lower reaches of the YRV, there is an anomalous cyclonic circulation accompanied by moisture divergence over the Arabian Sea and the Indian Peninsula. The moisture that produces the extreme precipitation events in the lower reaches of the YRV is from the southwest of the WPSH and the southerly wind over the South China Sea (see Fig. 7). It should be noted that if one standard deviation of EPF in the upper YRV is used to conduct the composite analysis, the results are still robust.

Acknowledgments The authors thank two reviewers for their constructive comments to improve our paper. This research was supported by the Special Fund for Public Welfare (Meteorology) under Grant No. GYHY200906018, the National Natural Science Foundation of China (Grant No. 41175071), Global Climate change research

National Basic Research Program of China (Grant No. 2010CB950304), and the Chinese Academy of Sciences under Grant No. KZCX2-YW-BR-14.

References

- Becker S, Hartmann H, Coulibaly M, Zhang Q, Jiang T (2008) Quasi periodicities of extreme precipitation events in the Yangtze River basin, China. *Theor Appl Climatol* 94(3–4):139–152. doi: [10.1007/s00704-007-0357-6](https://doi.org/10.1007/s00704-007-0357-6)
- Chen D, Gu L, Jiang XW (2010) Characteristics of large-scale circulation background of summer heavy rainfall in Sichuan during 1981–2000. *Trans Atmos Sci* 33(4):443–450 (in Chinese)
- Chen H, Sun J, Chen X, Zhou W (2012) CGCM projections of heavy rainfall events in China. *Int J Climatol* 32(3):441–450. doi: [10.1002/joc.2278](https://doi.org/10.1002/joc.2278)
- Ding YH, Sun Y, Wang ZY, Zhu YX, Song YF (2009) Inter-decadal variation of the summer precipitation in China and its association with decreasing Asian summer monsoon. Part II: possible causes. *Int J Climatol* 29(13):1926–1944. doi: [10.1002/joc.1759](https://doi.org/10.1002/joc.1759)
- Fan K (2006) Atmospheric circulation anomalies in the Southern Hemisphere and summer rainfall over Yangtze River Valley. *Chin J Geophys* 49(3):672–679 (in Chinese)
- Huang RH, Li WJ (1988) Influence of the heat source anomaly over the tropical western Pacific on the subtropical high over East Asia and its physical mechanism. *Chin J Atmos Sci* 12:107–116 (in Chinese)
- Jiang XW, Li YQ, Yang S, Wu RG (2011) Interannual and interdecadal variations of the South Asian and western Pacific subtropical highs and their relationships with Asian-Pacific summer climate. *Meteorol Atmos Phys* 113(3–4):171–180. doi: [10.1007/s00703-011-0146-8](https://doi.org/10.1007/s00703-011-0146-8)
- Jin LJ, Zhao P (2012) Observational and modeling studies of impacts of the South China Sea monsoon on the monsoon rainfall in the middle-lower reaches of the Yangtze River during summer. *Acta Meteorol Sin* 26(2):176–188. doi: [10.1007/s13351-012-0204-2](https://doi.org/10.1007/s13351-012-0204-2)
- Li CY, Pan J (2007) The interannual variation of the South China Sea summer monsoon trough and its impact. *Chin J Atmos Sci* 31(6):1049–1058 (In Chinese)
- Liao QH, Gao ST, Wang HJ, Tao SY (2004) Anomalies of the extratropical westerly jet in the north hemisphere and their impacts on east Asian summer monsoon climate anomalies. *Chin J Geophys* 47(1):10–18 (In Chinese)
- Liu YY, Ding YH (2009) Influence of the western North Pacific summer monsoon on the summer rainfall over the Yangtze River basin Chinese. *J Atmos Sci* 23(06):1225–1237 (In Chinese)
- Liu G, Zhang QY, Sun JQ (2008) The relationship between circulation and SST anomaly east of Australia and the summer rainfall in the middle and lower reaches of the Yangtze River. *Chin J Atmos Sci* 32(002):231–241 (In Chinese)
- Lu RY, Huang RH (1998) Influence of east Asia/Pacific teleconnection pattern on the interannual variations of the blocking highs over the northeastern Asia in summer. *Chin J Atmos Sci* 22(005):727–734 (In Chinese)
- Manton M, Della-Marta P, Haylock M, Hennessy K, Nicholls N, Chambers L, Collins D, Daw G et al (2001) Trends in extreme daily rainfall and temperature in southeast Asia and the south Pacific: 1961–1998. *Int J Climatol* 21(3):269–284. doi: [10.1002/joc.610](https://doi.org/10.1002/joc.610)
- Mao WS, Zhu KY, Huang KW, Zhou Q (2010) Characteristics of water vapor transport of summer precipitation anomalies in Sichuan–Chongqing region. *J Nat Resour* 25(2):280–290 (In Chinese)
- Nitta T (1987) Convective activities in the tropical western Pacific and their impact on the northern hemisphere summer circulation. *J Meteorol Soc Jpn* 65(3):373–390

- Plummer N, Salinger MJ, Nicholls N, Suppiah R, Hennessy KJ, Leighton RM, Trewin B, Page CM et al (1999) Changes in climate extremes over the Australian region and New Zealand during the twentieth century. *Clim Change* 42(1):183–202. doi:[10.1023/A:1005472418209](https://doi.org/10.1023/A:1005472418209)
- Qian YF, Zhang Y, Zhen YQ (2003a) Impacts of the Tibetan Plateau snow anomaly in winter and spring on precipitation in China in spring and summer. *Arid Meteorol* 21(3):1–7 (In Chinese)
- Qian YF, Zheng YQ, Zhang Y, Miao MQ (2003b) Responses of China's summer monsoon climate to snow anomaly over the Tibetan Plateau. *Int J Climatol* 23(6):593–613. doi:[10.1002/joc.901](https://doi.org/10.1002/joc.901)
- Ren GY, Feng GL, Yan ZW (2010) Progresses in observation studies of climate extremes and changes in mainland China. *Clim Environ* 15(4):337–353 (In Chinese)
- Su BD, Jiang T, Jin WB (2006a) Recent trends in observed temperature and precipitation extremes in the Yangtze River basin, China. *Theor Appl Climatol* 83(1–4):139–151. doi:[10.1007/s00704-005-0139-y](https://doi.org/10.1007/s00704-005-0139-y)
- Su BD, Jiang T, Ren GY, Chen ZH (2006b) Observed trends of precipitation extremes in the Yangtze river basin during 1960 to 2004. *Adv Clim Change Res* 2(001):9–14 (In Chinese)
- Sun JQ, Wang HJ, Yuan W (2009) A possible mechanism for the co-variability of the boreal spring Antarctic oscillation and the Yangtze river valley summer rainfall. *Int J Climatol* 29(9):1276–1284. doi:[10.1002/joc.1773](https://doi.org/10.1002/joc.1773)
- Sung MK, Kwon WT, Baek HJ, Boo KO, Lim GH, Kug JS (2006) A possible impact of the north Atlantic oscillation on the east Asian summer monsoon precipitation. *Geophys Res Lett* 33(21):L21713. doi:[10.1029/2006gl027253](https://doi.org/10.1029/2006gl027253)
- Tao SY, Zhu FK (1964) The 100-mb flow patterns in southern Asia in summer and its relation to the advance and retreat of the west Pacific subtropical anticyclone over the far east. *Acta Meteorol Sin* 34(4):385–395 (In Chinese)
- Tian BQ, Fan K (2012) Relationship between the late spring NAO and summer extreme precipitation frequency in the middle and lower reaches of the Yangtze river. *Atmos Ocean Sci Lett* 05(6):455–460
- Wang HJ, Fan K (2005) Central-north China precipitation as reconstructed from the Qing dynasty: signal of the Antarctic atmospheric oscillation. *Geophys Res Lett* 32:L24705. doi:[10.1029/2005GL024562](https://doi.org/10.1029/2005GL024562)
- Wang HJ, Fan K (2006) Relationship between the Antarctic oscillation and the western north Pacific typhoon frequency. *Chin Sci Bull* 52(4):561–565. doi:[10.1007/s11434-007-0040-4](https://doi.org/10.1007/s11434-007-0040-4)
- Wang HJ, Sun JQ, Chen HP, Zhu YL, Zhang Y, Jiang DB, Lang XM, Fan K et al (2012) Extreme climate in China: facts, simulation and projection. *Meteorol Z* 21(3):279–304. doi:[10.1127/0941-2948/2012/0330](https://doi.org/10.1127/0941-2948/2012/0330)
- Wu Z, Li J, Jiang Z, Ma T (2011) Modulation of the Tibetan Plateau snow cover on the ENSO teleconnections: from the east Asian summer monsoon perspective. *J Clim* 25(7):2481–2489. doi:[10.1175/jcli-d-11-00135.1](https://doi.org/10.1175/jcli-d-11-00135.1)
- Xu ZQ, Fan K (2012) Possible process for influences of winter and spring Indian ocean SST anomalies interannual variability mode on summer rainfall over eastern China. *Chin J Atmos Sci* 36(5):879–888 (In Chinese)
- Xue F, Wang HJ, He JH (2003) Interannual variability of Mascarene high and Australian high and their influences on summer rainfall over east Asia. *Chin Sci Bull* 48(5):492–497. doi:[10.1360/03tb9104](https://doi.org/10.1360/03tb9104)
- You QL, Kang SC, Aguilar E, Pepin N, Flugel WA, Yan YP, Xu YW, Zhang YJ et al (2011) Changes in daily climate extremes in China and their connection to the large scale atmospheric circulation during 1961–2003. *Clim Dyn* 36(11–12):2399–2417. doi:[10.1007/s00382-009-0735-0](https://doi.org/10.1007/s00382-009-0735-0)
- Yu LJ, Hu DX (2008) Role of snow depth in spring of Tibetan Plateau in onset of south China sea summer monsoon. *Chin J Geophys* 51(6):1682–1694 (In Chinese)
- Zhai PM, Zhang XB, Wan H, Pan XH (2005) Trends in total precipitation and frequency of daily precipitation extremes over China. *J Clim* 18(7):1096–1108. doi:[10.1175/JCLI-3318.1](https://doi.org/10.1175/JCLI-3318.1)
- Zhang Q, Wu GX (2001) The large area flood and drought over Yangtze river valley and its relation to the south Asia high. *Acta Meteorol Sin* 59(5):569–577 (In Chinese)
- Zhang Y, Li T, Wang B (2004) Decadal change of the spring snow depth over the Tibetan Plateau: the associated circulation and influence on the east Asian summer monsoon*. *J Clim* 17(14):2780–2793. doi:[10.1175/1520-0442\(2004\)017<2780:dcotss>2.0.co;2](https://doi.org/10.1175/1520-0442(2004)017<2780:dcotss>2.0.co;2)
- Zhou BT (2011) Linkage between winter sea surface temperature east of Australia and summer precipitation in the Yangtze river valley and a possible physical mechanism. *Chin Sci Bull* 56(17):1821–1827. doi:[10.1007/s11434-011-4497-9](https://doi.org/10.1007/s11434-011-4497-9)
- Zhu X, Bothe O, Fraedrich K (2011) Summer atmospheric bridging between Europe and east Asia: influences on drought and wetness on the Tibetan Plateau. *Quatern Int* 236(1–2):151–157. doi:[10.1016/j.quaint.2010.06.015](https://doi.org/10.1016/j.quaint.2010.06.015)